Global Localization Robust to GPS Outages using a Vertical Ladar

Maged Jabbour and Philippe Bonnifait

Heudiasyc UMR CNRS 6599, Université de Technologie de Compiègne
BP 20529 - 60205 COMPIEGNE cedex FRANCE - Tel. +33 (0)3 44 23 44 23 - Fax +33 (0)3 44 23 44 77
{maged.Jabbour, philippe.bonnifait}@hds.utc.fr ,

***Abstract* – This paper presents a localization strategy for vehicles in urban environments by mapping and updating natural landmarks provided by a 2D ladar (laser range scanner) when GPS data is unavailable or has a too poor quality because of multi-tracks or bad satellite visibility. The method relies on an approach that takes profit of successive passages in the same area.**

From the modelling point of view, a particularity of the method is due to the use of linear landmarks – sidewalk edges - which implies the management of topological connections. Real experiments carried out in real conditions prove the feasibility of this approach.

Index Terms – Localization, Sensor Fusion, Laser Range finder, GPS.

1 INTRODUCTION

Precise dynamic localization in urban areas is a key issue for many intelligent vehicles applications. Positioning systems often rely on the use of GPS (Global Positioning System)[6], dead-reckoning systems and GIS - Geographical Information Systems - information. Unfortunately, in urban areas, GPS suffers from satellite outages and multi-tracks, which can decrease significantly the precision of the estimated positions. The necessary conditions of having the minimum number satellites in the line of sight with a good geometry are rarely satisfied. A solution to this problem consists in adding Dead-Reckoning (DR) sensors like gyros and odometers. Unfortunately, GPS coupled with DR sensors may drift in urban areas if satellite outages last too long. Moreover, the precision of the DR-localization is often not good enough to reject aberrant GPS fixes due to multi-tracks.

Since several years, the use of additional exteroceptive sensors such as cameras [5, 8] and ladars [1, 18] is studied to enhance the precision, the availability and the integrity of localization. The use of such sensors implies the management of landmarks in maps. There are several approaches to this problem depending on the nature of the landmarks (artificial or natural) and on the map (provided by a third entity – a cartographer - or learned by the localization system). As well known in robotics, the problem of localizing a robot and building a map of its environment using artificial or natural landmarks is known as SLAM (Simultaneous Localization And Mapping). SLAM is the process that consists in localising a mobile robot and building in parallel a map of an unknown environment using only observations relative to the most relevant features detected by its sensors. Initial work on the subject was done by Smith and al. [15] who established statistical basis for relationships between landmarks and geometric uncertainty. In [7], it is shown that a generalized Kalman filter approach can theoretically solve the SLAM problem under white and Gaussian assumptions. SLAM can have various implementations, for example, in an outdoor environment or deal with 3-D mapping of urban areas with dynamic objects [10, 16]. Recent works deal with particle filters to handle multi-modality problems [13].

In case of using natural features for outdoor navigation in urban area, several works like [5, 14] propose to split the navigation in two stages: a learning stage in which a world model is built and navigation stages using this map. Its main difference with the SLAM approach is that the vehicle cannot be localized during the learning stage.

In this work, we propose a method that follows this paradigm. In a first passage, the vehicle is manually driven and an initial map corresponding to a ladar is built, even if there are regions that are in a permanent GPS masking. Then, at each next passage, the vehicle is able to localize itself and a map update is simultaneously performed. To illustrate this strategy, we consider in this paper the curbs of sidewalks that are detected by a vertical ladar. A metric/topological representation of the environment is used, where the natural landmarks are the sidewalk edges that are modelled by connected linear segments. Topological vectors are used to connect these linear landmarks. These vectors describe the belief of existence of each segment.

The paper is organized as follows. Next section describes the principle of the method. Section III presents the initial map building and its simultaneous update with the localization process. Section IV is dedicated to real experiments carried out with our experimental car.

2 PRINCIPLE OF THE METHOD

Let consider a vehicle equipped with a differential GPS receiver, a gyro and an odometer (called hereafter DR sensors). The fusion of GPS and DR sensors can reach a high level of performance, if the satellites visibility is good and if there is no multi-track. Our point of view is to use the GPS when it is *good* and coherent with the other sensors. In case of doubt, the current GPS fix is rejected. Obviously, such a strategy forces the GPS data to become more reliable but more intermittent. We propose to use a ladar to solve this problem by taking profit of successive passages of the vehicle in the

same areas. If the vehicle runs always on new roads, our method does not have interest.

During the first passage, the vehicle builds a map of the environment (the world model). During this stage, the localization is not improved by the ladar. So, during a GPS outage, the vehicle navigates with its DR sensors. The map is updated each next passage, simultaneously with the localization process. We think that the constraints imposed by the ladar associated with the map make the precision of the localization better: the ladar helps in correcting the drift of the dead-reckoned localization when GPS is unavailable. The more the vehicle navigates in the same area, the better the precision of the localization, since the map is continuously updated. Our method differs from usual SLAM, because of the initial map-building phase. This is due to the position of the ladar and due to the nature of the landmarks.

It is known that lateral drift of dead-reckoned navigation is larger than the longitudinal one [12]. Moreover, for autonomous navigation, the lateral precision is crucial. So, the ladar has to be used to detect as much as possible lateral landmarks. As in urban areas sidewalks present naturally this lateral feature, the ladar has been installed vertically in a way to detect lateral sidewalk edges. Figure 1 illustrates the prototype we have developed for this purpose. The horizontal and inclined setting proposed in [17] dedicated to road-boundary detection can be an alternative. Since the range of the ladar can reach easily several meters, the vehicle can navigate in the same area with a variable distance to the sidewalk: it is not obliged to follow exactly the same trajectory.

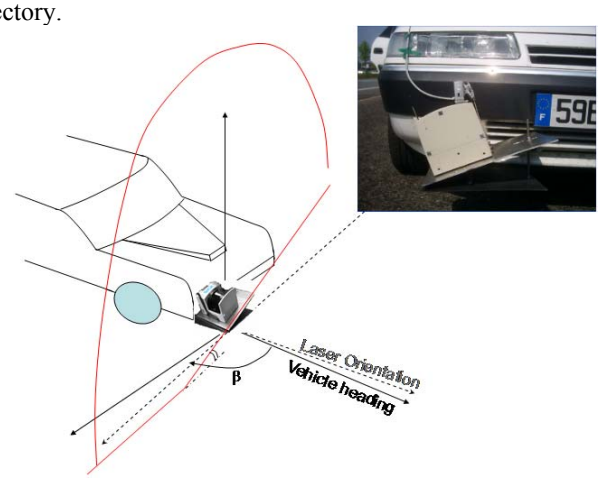

Fig. 1. Vertical ladar installed at the right front of our experimental vehicle.

3 IMPLEMENTATION

3.1 Map of the Ladar Landmarks

Maps can be either metric or topological. Metric maps contain landmarks or characteristic features with their global coordinates, while topological ones represent the environment by graphs where nodes correspond to significant places (or characteristics) and arcs to the different ways or transitions possible between these places. In other hybrid approaches [3], topological maps are augmented with metric information, and in [9], new hybrid metric maps that combine feature maps with any other metric representation are shown.

Let consider a map made up with a set of segments representing the sidewalk edges. Each segment is modelled by its two end-nodes and constitutes a linear landmark. The ladar observation is linked to the coordinates of the segment by a non-linear function (see Eq. 12). Since a curb is necessarily a polyline without any junction, the map is a set of polylines (Fig. 2).

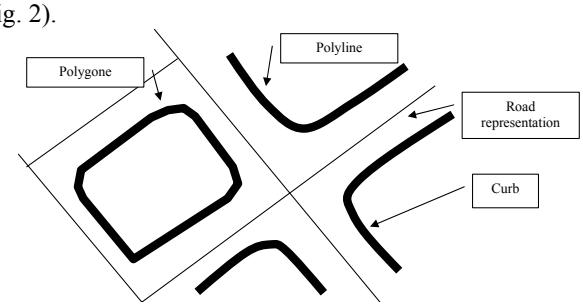

Fig. 2. Map made up with the road curbs

Let consider a polyline and let be S the vector made up with n segments. Each segment $[ij]$ is characterised by its two end-nodes (i,j) the coordinates of which are (x_i, y_i) and (x_j, y_j).

$$S = [x_1, y_1, \ldots, x_k, y_k, \ldots, x_{end}, y_{end}] \quad \text{size}(S) = 2n \times 1 \qquad (1)$$

The sidewalk may not exist on all the side of the road and the last node can be connected to the first point, if the curb is a polygon. Therefore, a connectivity vector B is associated to S.

$$B = [b_1, \ldots, b_n] \quad b_i \in [0..1] \quad \text{size}(B) = n \times 1 \qquad (2)$$

B elements can be interpreted as *believes* of having a link or a real connection between two successive nodes (the last term represents the connection between the last node and the first one).

Moreover, in order to be able to update the geometry of the map, a covariance matrix is associated to S. Its size is $(2n \times 2n)$

The representation of the map is hybrid: the probabilistic geometric representation derives from nodes coordinates (S vector) and its associated covariance, and the topological nature comes from the belief vector that characterizes connections between successive nodes.

3.2 Building an Initial Map

Because of the ladar installation, usual SLAM approach has little interest. Indeed, our vertical installation doesn't allow detecting the linear landmarks with a high redundancy. Therefore, we propose to consider the first passage on a road as a learning stage.

In order to build an initial map of the environment, it is necessary to have estimates of the pose of the vehicle, even if these estimates are really imprecise. Because GPS alone cannot localize continuously the vehicle especially in urban environments, the car is localized by fusing an odometer, a

gyrometer and GPS. If the GPS satellites signal is unavailable or not coherent, the evolution model provides a dead-reckoned pose estimate.

3.2.1 *Continuous Localization for Mapping*

Let us consider a car-like vehicle. The mobile frame is chosen with its origin *M* attached to the centre of the rear axle. The *x*-axis is aligned with the longitudinal axle of the car (see Fig. 3). The vehicle position is represented by Cartesian coordinates (x_k, y_k) of *M* in a world frame. The heading angle is denoted θ_k.

The evolution model of the vehicle is non-linear:

$$X_{v,k+1} = f(X_{v,k}, U_{v,k}, \gamma_k) + \alpha_{v,k} \quad (3)$$

Where $X_{v,k} = (x_k, y_k, \theta_k)$ is the vehicle state vector at instant k, $U_{v,k}$ the vector of the measured inputs (Δ_k, w_k), being respectively the elementary distance covered by the rear wheels and the elementary rotation of the mobile frame. $\alpha_{v,k}$ is the process noise and γ_k represents the measurement error of the inputs. $\alpha_{v,k}$ and γ_k are assumed to be uncorrelated and zero mean noises.

If the road is perfectly planar and horizontal, an evolution model can be expressed by:

$$\begin{cases} x_{v,k+1} = x_{v,k} + \Delta_k . cos(\theta_{v,k} + \frac{w_k}{2}) \\ y_{v,k+1} = y_{v,k} + \Delta_k . sin(\theta_{v,k} + \frac{w_k}{2}) \\ \theta_{v,k+1} = \theta_{v,k} + w_k \end{cases} \quad (4)$$

The values of Δ_k and w_k are computed using the ABS measurements of the rear wheels and a fibre optic gyrometer.

The fusion of GPS and odometry is done by an Extended Kalman Filter (EKF) which uses the prediction/update mechanism. In the prediction step, the car navigates using (4).

When a GPS position is available, a correction of the predicted pose is performed. It is necessary to verify the coherence of this position. For that, the normalized innovation squared which has a chi-square distribution is used: a distance d_m is computed between the GPS observation and the state vector. If the computed distance d_m is smaller than a threshold: $\chi^2(0.05,3)$ or $\chi^2(0.025,3)$, then the GPS measurement is assumed to be reliable and a correction on the predicted pose is performed. Otherwise, the dead-reckoned pose provided by the evolution model is kept.

3.2.2 *Map Building*

In this stage, the environment map is built using the vehicle pose and segmented data of the ladar (a split-and-merge mechanism similar to the one used in [2]).

Let (x_T, y_T) be the current coordinates of the laser centre **T**. They are computed using the following equations (see Fig. 3):

$$\begin{cases} x_T = x_M + t_x . \cos\theta + t_y . \sin\theta \\ y_T = y_M + t_x . \sin\theta - t_y . \cos\theta \end{cases} \quad (5)$$

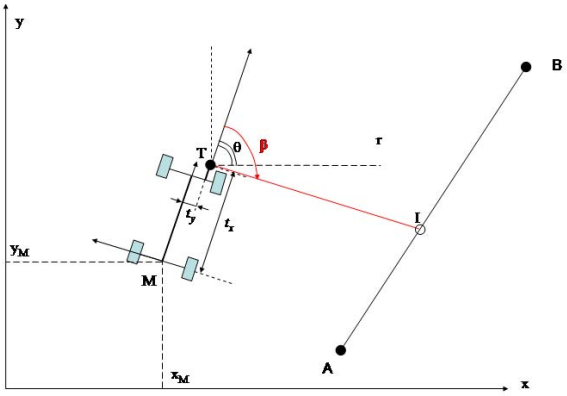

Fig. 3. Frames and observation measurement

The low-level sidewalk detection algorithm is based on the computation of slope variation of successive segments of the telemeter frame. The first slope value higher than a threshold corresponds to the edge of the sidewalk. This algorithm has been robustified to avoid spurious data such as people or obstacles between the equipped vehicle and the sidewalk edge. While the points (x_l, y_l) are contiguous, they are buffered. When a discontinuity appears, the sequence is segmented. The discontinuity can be due to the absence of a sidewalk or to a car parked, for example. The segmentation module returns a segment or a set of connected segments, depending on the level of segmentation specified.

Under the hypothesis of uncorrelated measurements, the covariance of the error of the map segments can be estimated by propagating the pose imprecision to each segmented point using a first order linearization [15].

The final step consists in estimating the values of vector *B* (see paragraph 3.1). A heuristic method consists in attributing a belief proportional to the number of raw points between 2 nodes. Regions that don't have sidewalk and those that contain parked cars are treated with the same manner: a null belief of existence is associated to them.

3.3 Localization and Map Updating

While the vehicle navigates in a learned area, simultaneously with the localization the map is updated. The used algorithm is based on generalized Kalman filtering and follows the prediction/estimation paradigm [7].

The global state vector *X* is composed by the vehicle state vector X_v, and the coordinates of the linear segments of the map *S*. So we have:

$$X = [X_v \quad S]^T \quad (6)$$

3.3.1 *Prediction*

The prediction step is written as follows:

$$X_{k+1} = F(X_k) + \alpha_k \quad (7)$$

Where $\boldsymbol{\alpha}_k$ is the vector of the process noise errors supposed to be white with zero mean. The evolution model can be developed as following:

$$\begin{bmatrix} X_{v,k+1} \\ S_{k+1} \end{bmatrix} = \begin{bmatrix} f() & 0_{n,2q} \\ 0_{2q,n} & I_{2q2q} \end{bmatrix} . \begin{bmatrix} X_{v,k} \\ S_k \end{bmatrix} + \alpha_k \qquad (8)$$

Where $f()$ is the odometric evolution model (See Eq. 3), $\boldsymbol{I_{2q,2q}}$ is the 2q-identity matrix (the linear landmarks are supposed stationary), $\boldsymbol{n}$ is the dimension of the vehicle state vector (here n=3), $\mathbf{0_{2q,\,n}}$ is a ($2.q$, n) zero matrix.

3.3.2 Correction: two update steps

Thanks to the exteroceptive sensors, it is now possible to estimate both the map and the vehicle pose. The observations are the GPS fix and the distance to the sidewalk edge:

$$Y = [x_{GPS} \quad y_{GPS} \quad r_{laser}]^T$$

As there are two distinct sources of observation, we chose to serialize the updating stages under the assumption that the noises are uncorrelated. The two exteroceptive sensors have been sampled and synchronized thanks to the GPS PPS signal at 5Hz. If the GPS data is present and coherent, a first update stage of the global state vector is done. Then, if a valid laser data corresponding to a sidewalk edge is present and coherent, a second updating stage occurs.

3.3.3 Segment Selection

Let us consider the Segment Selection problem which consists in extracting from the map the most likelihood segment using the predicted state vector. Let (x_{pred}, y_{pred}, θ_{pred}) be the predicted pose. ($x_{T,pred}$, $y_{T,pred}$) are determined by using (5). One can write the equation of line D $y = s.x + k$ passing by ($x_{T,pred}$, $y_{T,pred}$) and having $tan(\theta_{pred} + \beta)$ as slope (see Fig. 3). Let be the function

$$h(x,y) = \boldsymbol{y} - s.\boldsymbol{x} - k \qquad (9)$$

The line D intersects segment [AB] only if

$$h(x_A,y_A).h(x_B,y_B) \leq 0 \qquad (10)$$

To be a real sidewalk edge, the associated segment must also have a non-null belief of existence (higher than a threshold). If more than one segment satisfies these criteria, the nearest one is selected. As we will see in section 4, this simple nearest neighbour matching strategy gives good results.

3.3.4 Map and Pose Updating using the ladar

If the low-level process detects valid data corresponding to a sidewalk edge, the ladar update step can take place.

Let suppose here that the good segment [AB] has been selected from the map. The observation is the telemetric distance r to the sidewalk edge. r can be predicted by:

$$r_{pred} = \sqrt{(x_T - x_I)^2 + (y_T - y_I)^2} \qquad (11)$$

Where (x_T, y_T) are the predicted coordinates of the centre of the laser and (x_I, y_I) are the predicted coordinates of the intersection point of the laser beam with segment [AB] (see Fig. 3). The predicted distance r_{pred} is written as:

$$r_{pred} = \left| \frac{a.x_{pred} - y_{pred} + b}{\sqrt{a^2 + 1}.\cos(\theta_{pred} + \beta - \tan^{-1}(a) - \frac{\pi}{2})} \right| \qquad (12)$$

Where a and b are the parameters of the line passing by points A and B. The distance r_{pred} is a non-linear function of the vehicle's predicted pose and of the coordinates of segment [AB].

When a valid ladar observation is available, it is important to verify its coherence. The same kind of test applied on the GPS data in 3.2.1 is used here.

The belief value b_i is incremented each time the segment selection algorithm matches a ladar observation with the segment associated to the predicted pose. It is decremented if the segment selection module signals that there should be an observation of the sidewalk and there is not. It is checked that the value of each b_i stays in the interval [0 1]. There is an analogy with the method exposed in [7] to manage what is called "quality".

4 Experimental Results

Experiments have been performed in the downtown area of Compiègne using a SICK LMS291 at 75Hz with a 1 degree resolution and 8.1 m range, a KVH fibre optic gyro, an odometer input and a Trimble AgGPS 132 running with a geostationary differential correction (Omnistar).

4.1 Methodology to compute estimation errors

In order to compute estimation error, a PPK GPS receiver (a Trimble 5700) has been used with an offline computing software (Trimble Total Control - TTC). In order to simplify the computations, the Ag132 and the 5700 receivers have shared the same antenna.

TTC software uses the 5700 raw data recorded at 1 Hz during the trials. In order to get a better precision, the precise GPS ephemeredes data (SP3) have been downloaded from IGS (International GNSS service). We have also collected the ionosphere (IONEX).

For the error computation, only the PPK positions which had a few centimeters precision (known thanks to the observation of the residuals) were used as reference positions. Since it is important to distinguish between lateral and longitudinal errors, the computation has been achieved in the Frenet's frame.

4.2 Results

In the following, we propose to compare a localization system that uses GPS and DR only, with our complete system that uses in addition the ladar.

Figure 4 reports the map and successive vehicle positions after 4 passages. For more realism, the initial map has been built at a different date than the other tests. The segments corresponding to the sidewalks are plotted in thin (blue). The estimated vehicle positions are drawn in bold (black). The

gray shaded area is the area where the GPS was not available (urban canyon). In this test, the average speed was about 7 m/s.

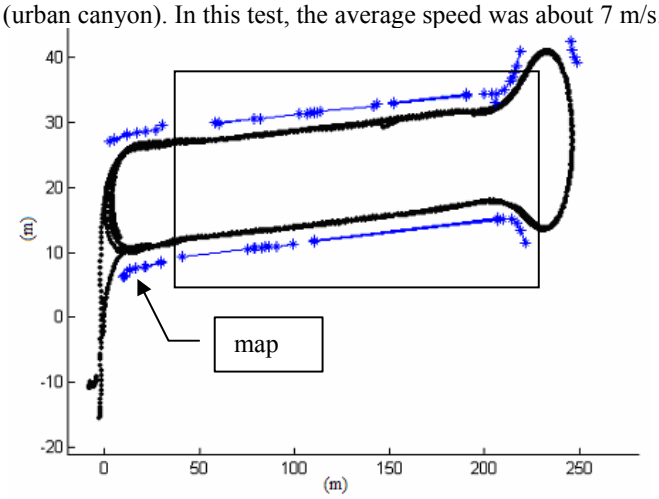

Fig. 4. Localization and map updating using GPS, DR and ladar.

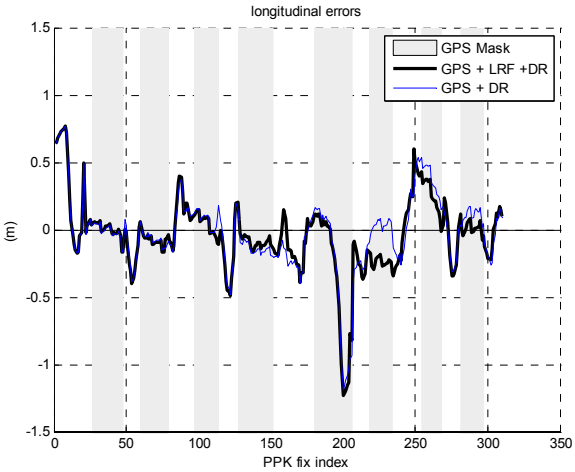

Fig. 5. Longitudinal Localization errors

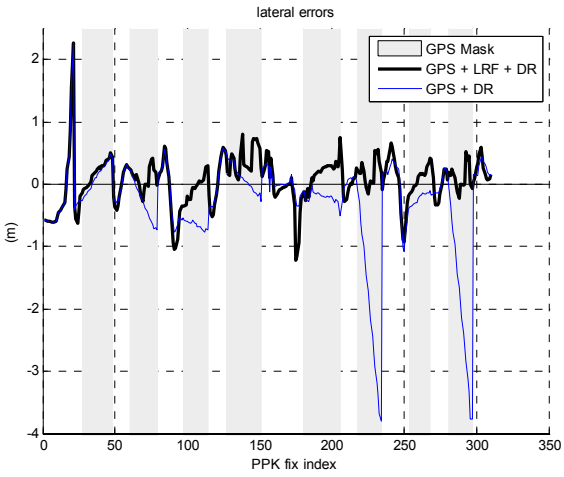

Fig. 6. Lateral Localization errors

Figures 5 and 6 show respectively the longitudinal and lateral errors of the localization algorithms. As explained before, the longitudinal and lateral errors are computed in the vehicle frame. The thin curve represents the errors in meters of the localization algorithm using GPS coupled with DR sensors. The bold one represents the localization error of the complete system which fuses GPS, ladar, and DR sensors. The gray bars show the GPS outages.

One can remark that the two methods have the same performance in the longitudinal direction. On the contrary, the complete system performs better in the lateral direction. These results indicate clearly that, when there is a GPS outage, the algorithm which uses the SLAM concept is very robust to lateral drift thanks to the fusion the ladar with the map and the DR sensors. The lateral error rarely exceeds 1 meter error, while the GPS+DR algorithm can drift significantly during GPS outages. When GPS is available, both localization processes give similar results.

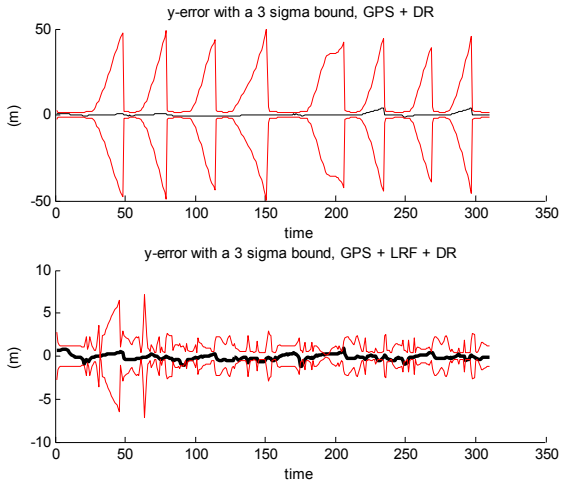

Fig. 7. y-errors with a 3σ estimated boundary

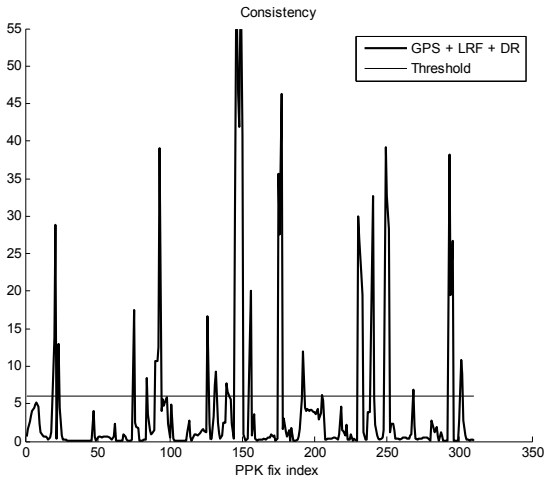

Fig. 8. Consistency of the estimated vehicle location

Figure 7 plots the y error for both algorithms with a 3σ estimated boundary. With the same notation as before, the thin curve represents the errors in meters of the localization algorithm using GPS coupled with DR sensors and the bold one represents the localization error of the complete system. The thin lines represent the 3σ estimated bound. The lateral error lacks a little bit of consistency. In this figure, the error is computed in the global frame and not in the Frenet's frame.

We observe here the consistency problem of an EKF-Based SLAM as in [4].

The consistency of the system was computed using the Normalized Estimation Error Squared (NEES), defined as:

$$D^2 = \begin{pmatrix} \hat{x} - x_{ppk} \\ \hat{y} - y_{ppk} \end{pmatrix}^T . P_{xy}^{-1} . \begin{pmatrix} \hat{x} - x_{ppk} \\ \hat{y} - y_{ppk} \end{pmatrix} \quad (13)$$

The consistency is checked using a chi-squared test: $D^2 < \chi^2(0.05,2)$. Figure 8 shows the consistency of the estimated vehicle position along its trajectory by the complete system. Its lack of consistency derives from the lack of consistency of the lateral localization which is too much optimistic. The localization consistency is 88,4% instead of 95% as we have used the following law: $\chi^2(0.05,2)$.

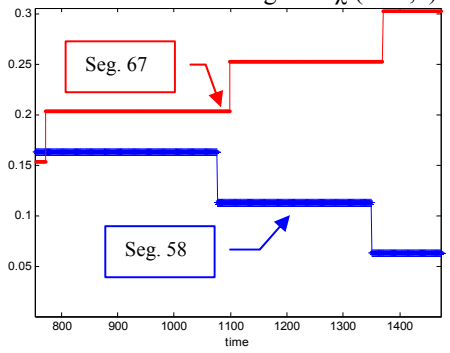

Fig. 9. Belief evolution of segments 58 and 67

Figure 9 plots the evolution of the belief of two segments after three passages. The belief of seg 58 decreases since this segment is not detected and since it has been selected from the map. On the contrary, the belief of seg 67 increases because in the map building stage the existence of a sidewalk was not trusty.

5 Conclusion

This paper has presented a novel approach to localize a vehicle in urban areas using the road edges. The main idea is to manage natural exteroceptive landmarks. When the area is unknown, the first passage consists in a learning stage and allows building an initial map. Afterwards, localization and map updating are performed conjointly thanks to a generalized Kalman filtering scheme.

We have focused on the use of a ladar installed vertically on a car to accurately detect sidewalk edges. In this case, the map contains segments used as linear landmarks. Their imprecision and belief of existence are handled especially to deal with blocks out of the laser beam.

Experimental results performed with our laboratory car indicate that this approach is relevant to navigation in real urban environment. Moreover, it can correct significantly the drift of DR sensors when GPS is blocked as proved by the experiments. Such situations occur frequently in urban environments. Unfortunately, we have noticed that the filter is difficult to tune and presents the weakness to be sometimes inconsistent. We think that it is due to the EKF approach sensible here to the high nonlinearity of the problem. The use of a UKF approach [11] should improve significantly the performance. Another important issue concerns the segment selection stage which is crucial to guaranty the convergence of the observer.

References

[1] I. Abuhadrous, F. Nashashibi, F. Goulette, C. Laurgeau, S. Ammoun, "Digitizing and 3D Modeling of Urban Environments and Roads Using Vehicle-Borne Laser Scanner System", 2004 IEEE/RSJ Int. Conf. on Int. Robots and Systems, Sept. 28 – Oct. 2, Sendai, Japan.

[2] G. Borges , M.-J. Aldon, "A Split-and-Merge Segmentation Algorithm for Line Extraction in 2-D Range Images", Int. Conf. on Pattern Recognition (ICPR'00) September 03 - 08, 2000 Barcelona, Spain.

[3] M.Bosse, P.Newman, J.Leonard, M.Soika, W.Felten, S.Teller: "An Atlas Framework for Scalable Mapping", Proc. IEEE Int. Conf. on Robotics and Automation (ICRA 2003), Sept. 14 -19, Taipei, Taiwan.

[4] J.A.Castellanos, J.Neira, J.D.Tardos, "Limits to the consistency of EKF-based SLAM", Proc. Of the Int. Symp. on Intelligent Autonomous Vehicles, Lisbon (Portugal), July 2004.

[5] F. Chausse, V. Voisin , J. Laneurit, R. Chapuis, "Centimetric localization of a vehicle combining vision and low cost GPS", Machine Vision Applications, MVA 2002, Dec. 11-13, Nara, Japan.

[6] S. Cooper and H. F. Durrant-Whyte, "A Kalman filter model for GPS navigation of land vehicles", in Proceedings of IEEE Int. Conf. on Robotics and Automation in San Diego, California, May 1994

[7] M. W. M. G. Dissanayake, P. Newman, S. Clark, H.F. Durrant-Whyte, M. Csorba, "A solution to the simultaneous localization and map building (SLAM) problem", IEEE Trans. on Robotics and Automation, 17, 3 (June 2001), pp. 229-241.

[8] A. Georgiev and P. K. Allen, "Localization Methods for a Mobile Robot in Urban Environments", IEEE Trans. on Robotics and Automation, V. 20, N. 5, pp. 851-864, Oct. 2004.

[9] J. Guivant, E..Nebot, J.Nieto, F.Masson, "Navigation and Mapping in Large Unstructured Environments" Int. Journal on Robotics Research, Vol.23, N.4, pp. 449-472, April 2004.

[10] D. Hähnel, D. Schulz, W. Burgard, "Map Building with Mobile Robots in Populated Environments". IEEE/RSJ Int. Conf. on Intelligent Robots and Systems (IROS), Oct. 2002, EPFL, Switzerland.

[11] S. J. Julier and J. K. Uhlmann. "A New Extension of the Kalman Filter to Nonlinear Systems". In Proc. of AeroSense: The 11th Int. Symp. on Aerospace/Defence Sensing, Simulation and Controls, April 1997.

[12] A. Kelly, "Linearized Error Propagation in Odometry", The Int. Journal of Robotics Research, Vol. 23, No. 2, February 2004.

[13] M. Montemerlo, S. Thrun, D. Koller, B. Wegbreit. "FastSLAM 2.0: An improved particle filtering algorithm for simultaneous localization and mapping that provably converges", Proc. of the Int. Joint Conf. on Artificial Intelligence (IJCAI) 2003, August 9-15, Acapulco, Mexico.

[14] E. Royer, J. Bom, M. Dhome, B. Thuillot, M. Lhuillier, F. Marmoiton, "Outdoor autonomous navigation using monocular vision". IEEE/RSJ International Conference on Intelligent Robots and Systems, pages 3395-3400, Edmonton, Canada, Aug. 2005.

[15] R. Smith, M. Self, P. Cheeseman, "Estimating Uncertainty Spatial Relationships in Robotics". 1988 Elsevier Science Publishers, Uncertainty in Artificial Intelligence, Vol 2. pp. 435-461.

[16] C.C. Wang, C. Thorpe, and S. Thrun, "Online simultaneous localization and mapping with detection and tracking of moving objects: Theory and results from a ground vehicle in crowded urban areas". IEEE Int. Conf. on Robotics and Automation (ICRA), May 12-17 2003, Taipei, Taiwan.

[17] W. S. Wijesoma, K. R. S. Kodagoda, and A. Balasuriya, "Road-Boundary Detection and Tracking Using Ladar Sensing", IEEE Trans. on Robotics and Automation, VOL. 20, NO. 3, pp.456-464 June 2004.

[18] H. Zhao, R. Shibasaki, "High Accurate Positioning and Mapping in urban area using laser range scanner", IEEE Intelligent Vehicle Symposium 2001, May 13-17, Tokyo, Japan.